



## Ab Initio Investigation of Interactions Between Dihalogenes and NCH Lewis Base

\*Makale Bilgisi / Article Info

Alındı/Received: 01.11.2024

Kabul/Accepted: 26.08.2025

Yayımlandı/Published: 03.02.2026

### Dihalojenler ve NCH Lewis Bazı Arasındaki Etkileşimlerin Ab Initio İncelemesi

Fatmagül TUNÇ

Artvin Coruh University, Vocational High School of Health Services, Artvin, Türkiye



© 2026 The Authors | Creative Commons Attribution-Noncommercial 4.0 (CC BY-NC) International License

#### Abstract

In this study, ab initio calculations (MP2/aug-cc-pVDZ) were employed to investigate the interaction dynamics, properties, and structures between dihalogenes (F<sub>2</sub>, Cl<sub>2</sub>, Br<sub>2</sub>, FCl, FBr, ClBr) as Lewis acids and NCH as a Lewis base. Electrostatic potential (ESP) analysis was conducted to identify  $\sigma$ -holes on the dihalogen systems. ESP analysis confirmed the presence of  $\sigma$ -holes on the dihalogenes, with the following order of increasing magnitude: FBr > FCl > ClBr > Br<sub>2</sub> > Cl<sub>2</sub> > F<sub>2</sub>. Interaction energies revealed that the FBr...NCH complex exhibited the strongest interaction, indicating its potential as a robust Lewis acid. NBO analysis demonstrated charge transfer from NCH to the dihalogen atoms, supporting the presence of significant noncovalent interactions. The Wiberg bond index (WBI) values ranged from 0.00 to 0.10, reinforcing the noncovalent nature of the interactions. The nature and origin of the interactions were investigated using quantum theory of atoms in molecules (QTAIM) and noncovalent interaction (NCI) index analyses. These analyses confirmed a closed-shell character, indicating attractive forces within the studied complexes.

**Keywords:** Dihalogenes; NCH; Ab Initio Calculations; ESP; QTAIM; NCI

#### Öz

Bu çalışmada, dihalojen (F<sub>2</sub>, Cl<sub>2</sub>, Br<sub>2</sub>, FCl, FBr, ClBr) Lewis asitleri ile NCH Lewis bazı arasındaki etkileşim dinamiklerini, özelliklerini ve yapılarını araştırmak için ab initio hesaplamalar (MP2/aug-cc-pVDZ) kullanılmıştır. Dihalojen sistemlerinde  $\sigma$ -hollerini belirlemek için elektrostatik potansiyel (ESP) analizi gerçekleştirilmiştir. ESP analizi, dihalojenlerde  $\sigma$ -hollerinin varlığını doğrulamış ve aşağıdaki artan büyüklük sıralamasını göstermiştir: FBr > FCl > ClBr > Br<sub>2</sub> > Cl<sub>2</sub> > F<sub>2</sub>. Etkileşim enerjileri, FBr...NCH kompleksinin en kuvvetli etkileşimi sergilediğini ve bunun güçlü bir Lewis asidi olma potansiyelini gösterdiğini ortaya koymuştur. NBO analizi, NCH'den dihalojen atomlarına doğru yük transferini destekleyerek önemli nonkovalent etkileşimlerin varlığını göstermiştir. Wiberg bağ indeksi (WBI) değerleri 0.00 ile 0.10 arasında değişmiş, etkileşimlerin nonkovalent doğasını pekiştirmiştir. Etkileşimlerin doğasını ve kökenini moleküllerdeki atomların kuantum teorisi (QTAIM) ve nonkovalent etkileşim (NCI) indeksi analizleri kullanılarak incelenmiştir. Bu analizler, incelenen kompleksler içinde çekici kuvvetlerin varlığını gösteren kapalı kabuk karakterini doğrulamıştır.

**Anahtar Kelimeler:** Dihalojenler; NCH; Ab Initio Hesaplamaları; ESP; QTAIM; NCI

#### 1. Introduction

Noncovalent interactions are gaining more attention due to their crucial roles across various domains, including crystal engineering (Gimeno et al. 2008, Munárriz et al. 2018), molecular recognition (Ariga et al. 2012, Mazik 2009), chemical reactions (Riel et al. 2019, Choudhuri et al. 2020), adsorption (Malhotra et al. 2019), and biological functions (Stasyuk et al. 2017). Exploring the origins and characteristics of these interactions, as well as their influence on molecular system control, is viewed as a key milestone in contemporary chemistry. Among these interactions,  $\sigma$ -hole interactions stand out for their significance in ligand-acceptor relationships (Mani and Arunan 2014, Mahmoudi et al. 2016), self-assembly processes (Zeng et al. 2020), and anion recognition (Lim and Beer 2018).

The concept of the  $\sigma$ -hole was introduced by Politzer and others (Murray et al. 2012, Politzer et al. 2008, Murray et al. 2007) to explain halogen bonding (Clark et al. 2007). Since then, it has been broadened to include various noncovalent interactions involving elements from groups IV to VII. These interactions occur between electron-deficient regions, or  $\sigma$ -holes, located around tetrel (Scheiner 2020, Scheiner 2021), pnictogen (Zhuo et al. 2015, Bauzá et al. 2012, Alkorta et al. 2014), chalcogen (Guo et al. 2015, Varadwaj et al. 2019, Wang et al. 2009), and halogen atoms (Riley et al. 2011, Cavallo et al. 2016, Hauchecorne et al. 2010, Ibrahim et al. 2022). These  $\sigma$ -holes can engage with nucleophiles such as  $\pi$ -systems (Ibrahim et al. 2021, Ibrahim et al. 2019), anions (McDowell and Joseph 2014, Clark and Heßelmann 2018), or radicals (Li et al. 2014). The  $\sigma$ -hole typically aligns with

the direction of the  $\sigma$ -bond and its size tends to correlate with the electronegativity of the donor atom as well as the nature of its covalent bonds with neighboring atoms (Hennemann et al. 2012, Politzer and Murray 2017). Additionally, the strength of  $\sigma$ -hole interactions tends to increase when the nucleophiles Lewis basicity is heightened (Politzer and Murray 2013).

The halogen bond is a type of  $\sigma$ -hole interaction where the halogen acts as a Lewis acid, effectively functioning as an "electron acceptor" that attracts Lewis bases. This behavior may seem counterintuitive, given that halides typically carry a negative charge. However, the distribution of electron density around the halogen creates a  $\sigma$ -hole, allowing it to engage in bonding. The strength of the halogen bond is influenced by the angle between the D-X...A (D: Donor, X: Halogens, and A: Acceptor) components, with an optimal angle of  $180^\circ$ , which indicates a preference for a linear arrangement. This linear geometry is a defining characteristic of halogen bonding (Politzer et al. 2007, Clark et al. 2007, Politzer et al. 2010, Eskandari and Zariny 2010, Shields et al. 2010, Clark 2013).

This study seeks to explore the characteristics of  $\sigma$ -hole interactions within the XY...NCH complex systems, where XY represents F<sub>2</sub>, Cl<sub>2</sub>, Br<sub>2</sub>, FCl, FBr, and ClBr. A series of quantum mechanical calculations were performed, including geometrical optimization, electrostatic potential (ESP) maps, surface electrostatic potential extrema ( $V_{s,max}$ ), interaction energy assessment, as well as analyses using natural bond orbital (NBO) and wiberg bond index (WBI) methods. To gain deeper insights, the quantum theory of atoms in molecules (QTAIM) and the noncovalent interaction (NCI) index were utilized to provide a topological analysis of the nature of the selected interactions.

## 2. Materials and Methods

All computations were conducted using Gaussian 09, employing the MP2 method and the aug-cc-pVDZ basis set (Frisch et al. 2009). The geometric minima of the complexes were confirmed by the absence of imaginary frequencies. The interaction energies have been addressed using the standard counterpoise correction (CP) method proposed by Boys and Bernardi for the correction of the basis set superposition error (BSSE) (Boys and Bernardi 1970). NBO analysis was conducted with Gaussian 09 to investigate orbital interactions between occupied and unoccupied orbitals, as well as to calculate the WBI (Glendening et al. 2001). Additional analyses, including ESP, QTAIM and NCI analyses were carried out using Multiwfn 3.8(dev) software (Lu and

Chen 2012), with visualization performed through Visual Molecular Dynamics (VMD) software (Humphrey et al. 1996).

## 3. Results and Discussions

### 3.1. ESP and $V_{s,max}$ Calculations

ESP analysis is a valuable approach for gaining both qualitative and quantitative insights into the nucleophilic and electrophilic characteristics of the chemical systems being examined. This approach allows for a deeper understanding of the interactions at play within these systems (Weiner et al. 1982, Murray and Politzer 2011). Figure 1 presents the molecular electrostatic potential maps for all analyzed systems, highlighting the values of the maximum electrostatic potential ( $V_{s,max}$ ) at the  $\sigma$ -hole for the Lewis acids (LAs) F<sub>2</sub>, Cl<sub>2</sub>, Br<sub>2</sub>, FCl, FBr, and ClBr, as well as the minimum electrostatic potential ( $V_{s,min}$ ) at the nitrogen atom of the nucleobase (NCH) Lewis base (LB).

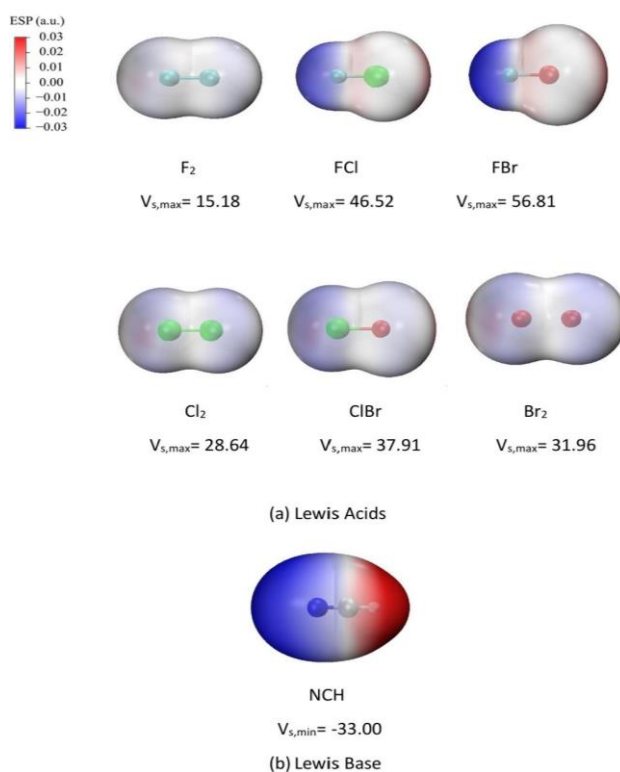


Figure 1. ESP maps of the investigated (a) XY LAs and (b) NCH LB molecules. ESP varies from -0.03 (blue) to 0.03 au (red). Values of  $V_{s,min}/V_{s,max}$  are given in kcal/mol.

The ESP maps shown in Figure 1 revealed a prominent blue region, indicative of negative ESP, located on the surface of the nitrogen atom in the examined LB. This observation underscores the potential for attractive interactions between the defined molecules and the LAs. Additionally, a red region, representing positive ESP, was observed opposite the  $\sigma$ -hole in the analyzed molecules. The magnitude of  $V_{s,max}$  at the  $\sigma$ -hole increased in the following order: FBr > FCl > ClBr > Br<sub>2</sub> > Cl<sub>2</sub> > F<sub>2</sub>, with

corresponding values of 56.81, 46.52, 37.91, 31.96, 28.64, and 15.18 kcal/mol, respectively.

### 3.2. Geometric parameters and interaction energies

Table 1 presents the principal geometric parameters and interaction energies for the systems under investigation, as determined using the MP2/aug-cc-pVDZ method, with corrections for basis set superposition error (BSSE) applied.

Table 1. Selected geometric parameters (Y: F, Cl, Br) and interaction energies

	R(Y...N) (Å)	E <sub>int</sub> (BSSE) (kcal/mol)
F <sub>2</sub> ...NCH	2.66238	-1.25
FCI...NCH	2.60493	-4.94
FBr...NCH	2.53563	-7.07
Cl <sub>2</sub> ...NCH	2.81119	-2.86
ClBr...NCH	2.73808	-4.48
Br <sub>2</sub> ...NCH	2.79225	-3.67

As indicated in Table 1, the complexes exhibited a propensity for noncovalent interactions, evidenced by their negative interaction energies (E<sub>int</sub>(BSSE)). The interaction energies became increasingly negative as the  $\sigma$ -hole size increased, following the order: FBr > FCI > ClBr > Br<sub>2</sub> > Cl<sub>2</sub> > F<sub>2</sub>, with values of -7.07, -4.94, -4.48, -3.67, -2.86, and -1.25 kcal/mol, respectively. The findings obtained in this study are in agreement with theoretical studies on similar  $\sigma$ -hole interactions reported in the literature. The conclusion that the FBr...NCH complex exhibits a strong interaction has also been similarly reported in a study published in the journal *Molecules*. In that study, the interaction energy of the FBr...NCH complex was calculated to be approximately -7.1 kcal/mol, which is in close agreement with the energy calculated in the present study (Murray 2024). Notably, the highest negative interaction energy corresponded to the smallest Y...N distance among the studied complexes. The findings indicated a strong relationship between the size of the  $\sigma$ -hole and the E<sub>int</sub>(BSSE), evidenced by a high correlation coefficient (R<sup>2</sup> = 0.9786), as illustrated in Figure 2.

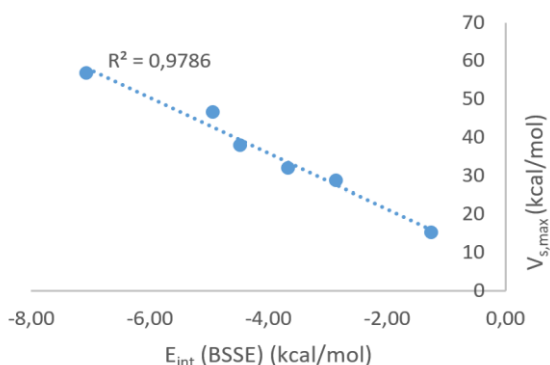


Figure 2. Linear relationship between E<sub>int</sub> (BSSE) interaction energy and V<sub>s,max</sub>

### 3.3. NBO analysis

NBO analysis is a powerful technique for exploring both intra- and intermolecular bonding as well as understanding charge transfer and conjugative interactions in molecular systems. This approach focuses on the interactions between donor and acceptor orbitals, incorporating stabilization energies derived from second-order perturbation theory. By analyzing the second-order Fock matrix, one can assess the interactions between these donor and acceptor orbitals within the NBO framework. These interactions represent the redistribution of electron density from the localized NBOs of the Lewis structure to the vacant non-Lewis orbitals. The stabilization energy, E(2), associated with the delocalization between a donor orbital i and an acceptor orbital j is calculated using the following equation:

$$E(2)(i \rightarrow j) = \frac{q_i F_{ij}^2}{\epsilon_j - \epsilon_i} \quad (1)$$

where  $q_i$  is the donor occupancy,  $F_{ij}$  is the Fock matrix element between the donor and acceptor, and  $\epsilon_j$  and  $\epsilon_i$  are the orbital energies of the acceptor and donor, respectively (Reed et al. 1988).

In the NBO analysis, the large E(2) values signified intense interactions between electron donors and acceptors. Specifically, all interactions considered in this study involve lone pair (LP)  $\rightarrow \sigma^*(X-Y)$  transitions, and the corresponding E(2) values associated with the nitrogen lone pair showed an increasing trend across all complexes. Higher E(2) values suggest more robust interactions between electron donors and improved conjugation throughout the system. As presented in Table 2, the FBr...NCH complex exhibited an E(2) value of 19.26 kcal/mol, indicating significant stabilization of the molecular structure. A comparative analysis of the E(2) values suggests that the stabilization order correlates positively with the interaction energy.

Table 2. NBO parameters of all complexes

	E(2) (kcal/mol)	WBI
F <sub>2</sub> ...NCH	0.86	0.0047
FCI...NCH	9.10	0.0432
FBr...NCH	19.26	0.0868
Cl <sub>2</sub> ...NCH	3.40	0.0161
ClBr...NCH	8.54	0.0357
Br <sub>2</sub> ...NCH	6.71	0.0281

The WBI serves as a relative measure of bond strength between two atoms, providing insights into the nature of various noncovalent interactions, such as pnictogen and halogen bonds. The observed WBI values, which range from 0.00 to 0.10, further substantiate the noncovalent character of these interactions. As outlined in Table 2, the WBI values for all considered complexes are below 0.10,

reinforcing the conclusion that these complexes exhibit predominantly noncovalent interactions.

### 3.4. QTAIM analysis

QTAIM has proven to be a valuable tool for understanding interactions in molecular complexes (Bader 1985). In this study, QTAIM was employed to investigate  $\sigma$ -hole interactions by identifying bond critical points (BCPs) and bond paths (BPs). Within this framework, the nature of closed-shell interactions was assessed by analyzing several features associated with the BCPs, such as electron density ( $\rho_b$ ), the Laplacian of the electron density ( $\nabla^2\rho_b$ ), and total energy density ( $H_b$ ). This approach facilitated a detailed examination of the interactions present in the system. Figure 3 illustrates the identified BCPs and BPs within the complexes under investigation. The values for  $\rho_b$ ,  $\nabla^2\rho_b$ , and  $H_b$  related to the dihalogen...NCH complexes are presented in Table 3.

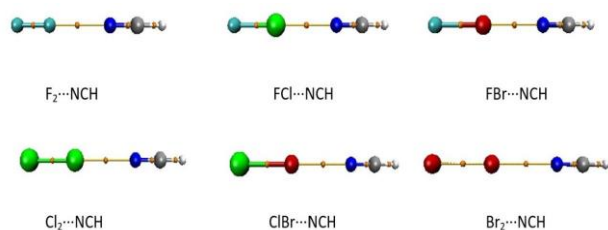


Figure 3. Quantum theory of atoms in molecules (QTAIM) diagrams of the optimized studied complexes

Table 3. Topological parameters, including the electron density ( $\rho_b$  (au)), Laplacian ( $\nabla^2\rho_b$  (au)), and total energy density ( $H_b$  (au)) at bond critical points (BCPs) of the optimized complexes

	$\rho_b$	$\nabla^2\rho_b$	$H_b$
F <sub>2</sub> ...NCH	0.0115	0.0513	0.0015
FCl...NCH	0.0228	0.0916	0.0028
FBr...NCH	0.0309	0.1101	0.0013
Cl <sub>2</sub> ...NCH	0.0154	0.0602	0.0023
ClBr...NCH	0.0210	0.0754	0.0020
Br <sub>2</sub> ...NCH	0.0191	0.0682	0.0020

Analysis of the data in Table 3 revealed that all studied complexes exhibit positive values for  $\rho_b$ ,  $\nabla^2\rho_b$ , and  $H_b$ , which indicate the closed-shell characteristics of the interactions examined. Similarly, in a study conducted by Ibrahim and Moussa (2020) on halogen-halogen complexes, QTAIM analysis revealed that the electron density, Laplacian, and total energy density at the bond critical points were all positive. These findings are consistent with the QTAIM results obtained for the complexes in the present study. Moreover, a robust correlation between the  $\rho_b$  values and the interaction energy trends was observed, with a high coefficient of determination ( $R^2$ ) of 0.9909, as demonstrated in Figure 4. This finding reinforces the closed-shell nature of the studied complexes.

### 3.5. NCI analysis

The noncovalent interaction-based reduced density gradient (NCI-RDG) index, which is based on noncovalent interactions, provides an important viewpoint on the nature of intermolecular interactions (Johnson et al. 2010, Munárriz et al. 2018). This index relies on the electron density ( $\rho$ ) and its derivatives to analyze these interactions. For complexes formed between dihalogens and Lewis bases, two-dimensional plots were created that depict the reduced density gradient (RDG) versus the sign of the second derivative of the electron density ( $sign(\lambda_2)\rho$ ). Additionally, three-dimensional NCI diagrams were generated to illustrate the isosurfaces of noncovalent interactions, as shown in Figures 5 and 6.

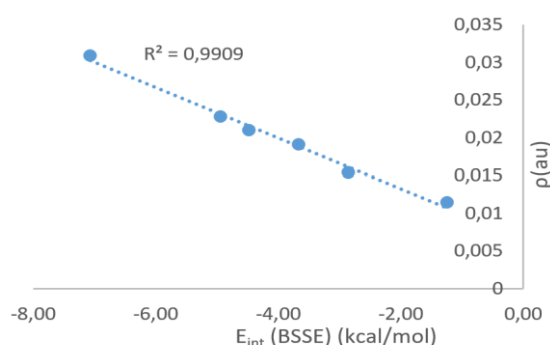


Figure 4. Linear relationship between  $E_{int}$  (BSSE) interaction energy and  $\rho_b$  electron density

In Figure 5, the blue region, corresponding to the range  $-0.05 < sign(\lambda_2)\rho < -0.03$ , indicates the presence of strong intermolecular interactions. Conversely, the green region, observed within the range  $-0.03 < sign(\lambda_2)\rho < 0.01$ , signifies weak intermolecular interactions, primarily highlighting van der Waals (vdW) interactions characterized by low electron densities. Values of  $sign(\lambda_2)\rho$  greater than 0.01 are associated with steric effects. Notably, the FBr...NCH complex exhibits a larger negative peak, which may be interpreted as a more stable structural deviation within this system.

As evident in Figure 6, a dark blue region was observed in the FBr...NCH complex, indicating an attractive interaction. In the resonance structures of certain complexes, the interaction is represented by a bicolored (blue/red curved) region, signifying a mixed interaction type involving both attraction and repulsion. Additionally, blue and red circles were identified in the FBr...NCH complex, indicating the presence of partially covalent bonds. Furthermore, green regions may indicate weak or transitional interaction zones and red regions representing strong steric effects are also visible in Figure 6.

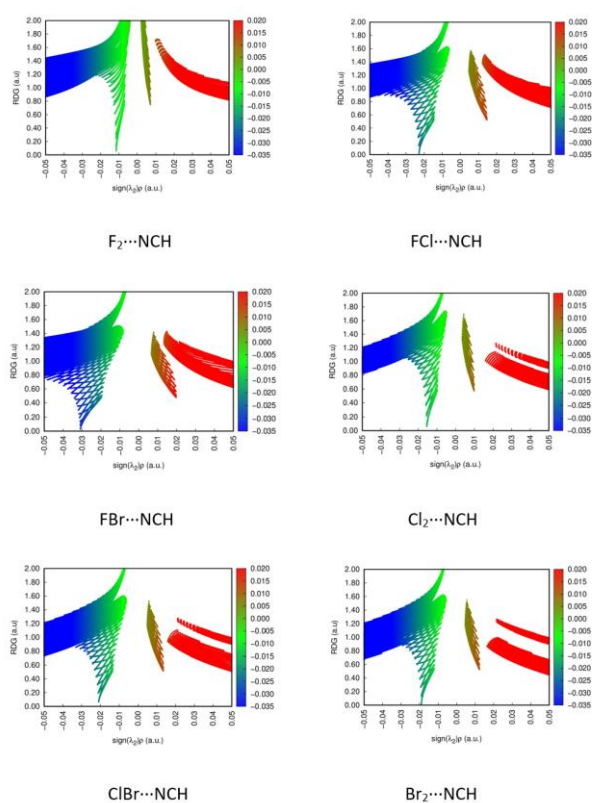


Figure 5. 2D NCI plots of the dihalogens...NCH complexes

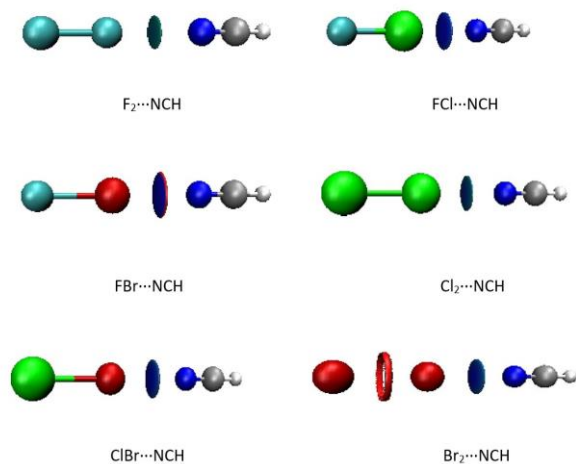


Figure 6. 3D NCI plots of the dihalogens...NCH complexes

#### 4. Conclusions

The ESP analysis, alongside geometrical, energetic, and advanced computational methods such as NBO, WBI, QTAIM, and NCI analyses, has provided a comprehensive understanding of the noncovalent interactions between the dihalogens LAs and the NCH LB in the examined complexes. The ESP maps revealed distinct regions of electrostatic potential, with a clear trend in the  $V_{s,max}$  correlating with the strength of interaction energies among the LAs. The results demonstrated that larger  $\sigma$ -holes facilitate stronger interactions. This is evidenced by

increasingly negative interaction energies, confirming a robust relationship between  $\sigma$ -hole size and interaction strength.

The NBO analysis highlighted significant electron density transfer between the nitrogen atom of the LB and the  $\sigma^*(X-Y)$  antibonding orbitals, particularly in the FBr...NCH complex, which exhibited the highest  $E(2)$  value and stabilization. The WBI values further emphasized the noncovalent nature of these interactions, remaining consistently low across all complexes.

Moreover, the QTAIM analysis reinforced the closed-shell character of the interactions, with strong correlations observed between the electron density ( $\rho_b$ ) and interaction energy patterns. This closed-shell characteristic is essential for understanding the stability of these complexes. The NCI analysis provided additional insights into the intermolecular interactions. It distinguished between strong and weak interactions and highlighted the presence of steric effects in the FBr...NCH complex.

Overall, this multifaceted analysis underscores the importance of electrostatic interactions in governing the behavior of Lewis acid-base complexes, with the results contributing valuable insights into their structural and energetic properties. These findings have implications for further studies in molecular interactions. They may inform the design of new chemical systems with tailored properties based on the observed noncovalent interactions.

#### Acknowledgements

The numerical calculations reported in this paper were fully/partially performed at TUBITAK ULAKBIM. High Performance and Grid Computing Center (TRUBA resources).

#### Declaration of Ethical Standards

The authors declare that they comply with all ethical standards.

#### Credit Authorship Contribution Statement

Author-1: Preparation of resources, methodology development, interpreting results, and writing the manuscript.

#### Declaration of Competing Interest

The authors have no conflicts of interest to declare regarding the content of this article.

#### Data Availability Statement

The authors declare that the primary data supporting the findings of this study are available within the article.

## 5. References

- Ariga, K., Ito, H., Hill, J. P. & Tsukube, H., 2012. Molecular recognition: From solution science to nano/materials technology. *Chemical Society Reviews*, 41, 5800–5835. <https://doi.org/10.1039/C2CS35162E>
- Alkorta, I., Elguero, J. & Solimannejad, M., 2014. Single electron pnictogen bonded complexes. *The Journal of Physical Chemistry A*, 118, 947–953. <https://doi.org/10.1021/jp412144r>
- Bader, R. F. W., 1985. Atoms in molecules. *Accounts of Chemical Research*, 18, 9-15. <https://doi.org/10.1021/ar00109a003>
- Bauzá, A., Quiñonero, D., Deyà, P.M. & Frontera, A., 2012. Pnictogen- $\pi$  complexes: Theoretical study and biological implications. *Physical Chemistry Chemical Physics*, 14, 14061–14066. <https://doi.org/10.1039/C2CP42672B>
- Boys, S. F. & Bernardi, F., 1970. The calculation of small molecular interactions by the differences of separate total energies. Some procedures with reduced errors. *Molecular Physics*, 19, 553-566. <https://doi.org/10.1080/00268977000101561>
- Cavallo, G., Metrangolo, P., Milani, R., Pilati, T., Priimagi, A., Resnati, G. & Terraneo, G., 2016. The halogen bond. *Chemical Reviews*, 116, 2478–2601. <https://doi.org/10.1021/acs.chemrev.5b00484>
- Choudhuri, K., Pramanik, M. & Mal, P., 2020. Noncovalent interactions in C-S bond formation reactions. *The Journal of Organic Chemistry*, 85, 11997–12011. <https://doi.org/10.1021/acs.joc.0c01534>
- Clark, T., Hennemann, M., Murray, J. S. & Politzer, P., 2007. Halogen bonding: the  $\sigma$ -hole. *Proceedings of "Modeling interactions in biomolecules II"*, Prague, September 5th-9th, 2005. *Journal of Molecular Modeling*, 13, 291–296. <https://doi.org/10.1007/s00894-006-0130-2>
- Clark, T., 2013.  $\sigma$ -Holes. *WIREs Computational Molecular Science*, 3, 13–20. <https://doi.org/10.1002/wcms.1113>
- Clark, T. & Heßelmann, A., 2018. The coulombic  $\sigma$ -hole model describes bonding in  $CX_3I \cdots Y$  complexes completely. *Physical Chemistry Chemical Physics*, 20, 22849–22855. <https://doi.org/10.1039/C8CP03079K>
- Eskandari, K. & Zariny, H., 2010. Halogen bonding: A lump-hole interaction. *Chemical Physics Letters*, 492, 9–13. <https://doi.org/10.1016/j.cplett.2010.04.021>
- Frisch, M. J., Trucks, G. W., Schlegel, H. B., Scuseria, G. E., Robb, M. A., Cheeseman, J. R., Scalmani, G., Barone, V., Mennucci, B., Petersson, G. A., et al., 2009. Gaussian 09, Revision C.01, Gaussian, Inc., Wallingford CT.
- Gimeno, N., Ros, M.B., Serrano, J. L. & De la Fuente, M.R., 2008. Noncovalent interactions as a tool to design new bent-core liquid-crystal materials. *Chemistry of Materials*, 20, 1262–1271. <https://doi.org/10.1021/cm701930b>
- Glendening, E. D., Badenhoop, J. K., Reed, A. E., Carpenter, J. E., Bohmann, J. A., Morales, C. M. & Weinhold, F., 2001. Natural Bond Orbital Program, Version 5.0, Theoretical Chemistry Institute, University of Wisconsin, Madison.
- Guo, X., An, X. & Li, Q., 2015. Se $\cdots$ N chalcogen bond and Se $\cdots$ X halogen bond involving F<sub>2</sub>C=Se: Influence of hybridization, substitution, and cooperativity. *The Journal of Physical Chemistry A*, 119, 3518–3527. <https://doi.org/10.1021/acs.jpca.5b00783>
- Hauchecorne, D., van der Veken, B. J., Moiana, A. & Herrebout, W. A., 2010. The C–Cl $\cdots$ N halogen bond, the weaker relative of the C–I and C–Br $\cdots$ N halogen bonds, finally characterized in solution. *Chemical Physics*, 374, 30–36. <https://doi.org/10.1016/j.chemphys.2010.06.004>
- Hennemann, M., Murray, J. S., Politzer, P., Riley, K. E. & Clark, T., 2012. Polarization-induced  $\sigma$ -holes and hydrogen bonding. *Journal of Molecular Modeling*, 18, 2461–2469. <https://doi.org/10.1007/s00894-011-1263-5>
- Humphrey, W., Dalke, A., & Schulten, K. (1996). VMD – Visual Molecular Dynamics. *Journal of Molecular Graphics*, 14, 33–38. [https://doi.org/10.1016/0263-7855\(96\)00018-5](https://doi.org/10.1016/0263-7855(96)00018-5)
- Ibrahim, M. A. A., Ahmed, O. A. M., Moussa, N. A. M., El-Taher, S. & Moustafa, H., 2019. Comparative investigation of interactions of hydrogen, halogen and tetrel bond donors with electron-rich and electron-deficient  $\pi$ -systems. *RSC Advances*, 9, 32811–32820. <https://doi.org/10.1039/C9RA08007D>
- Ibrahim, M. A. A., & Moussa, N. A. M. (2020). Unconventional Type III halogen $\cdots$ halogen interactions: A quantum mechanical elucidation of  $\sigma$ -hole $\cdots$  $\sigma$ -hole and di- $\sigma$ -hole interactions. *ACS Omega*, 5(36), 21824–21835. <https://doi.org/10.1021/acsomega.0c03069>
- Ibrahim, M. A. A., Ahmed, O. A. M., El-Taher, S., Al-Fahemi, J. H., Moussa, N. A. M. & Moustafa, H., 2021. Cospatial  $\sigma$ -hole and lone pair interactions of square-pyramidal pentavalent halogen compounds with  $\pi$ -systems. *ACS Omega*, 6, 3319–3329. <https://doi.org/10.1021/acsomega.0c05795>
- Ibrahim, M. A. A., Saeed, R. R. A., Shehata, M. N. I., Ahmed, M. N., Shawky, A. M., Khowdiary, M. M., Elkheed, E. B., Soliman, M. E. S. & Moussa, N. A. M.,

2022. Type I-IV halogen...halogen interactions: A comparative theoretical study in halobenzene...halobenzene homodimers. *International Journal of Molecular Sciences*, 23, 3114.  
<https://doi.org/10.3390/ijms23063114>
- Johnson, E. R., Keinan, S., Mori-Sánchez, P., Contreras-García, J., A. Cohen, A. J. & Yang, W., 2010. Revealing noncovalent interactions. *Journal of the American Chemical Society*, 132, 6498–6506.  
<https://doi.org/10.1021/ja100936w>
- Li, Q., Guo, X., Yang, X., Li, W., Cheng, J. & Li, H. B. A., 2014. A  $\sigma$ -hole interaction with radical species as electron donors: Does single-electron tetrel bonding exist? *Physical Chemistry Chemical Physics*, 16, 11617–11625.  
<https://doi.org/10.1039/C4CP01209G>
- Lim, J. Y. C. & Beer, P.D., 2018. Sigma-hole interactions in anion recognition. *Chem*, 4, 731–783.  
<https://doi.org/10.1016/j.chempr.2018.02.022>
- Lu, T. & Chen, F., 2012. Multiwfn: A multifunctional wavefunction analyzer. *Journal of Computational Chemistry*, 33, 580–592,  
<https://doi.org/10.1002/jcc.22885>
- Mahmoudi, G., Bauzá, A., Amini, M., Molins, E., Mague, J. T. & Frontera, A., 2016. On the importance of tetrel bonding interactions in lead(ii) complexes with (iso)nicotinohydrazide based ligands and several anions. *Dalton Transactions*, 45, 10708–10716.  
<https://doi.org/10.1039/C6DT01947A>
- Malhotra, D., Cantu, D. C., Koech, P. K., Heldebrant, D. J., Karkamkar, A., Zheng, F., Beard, M. D., Rousseau, R. & Glezakou, V. A., 2019. Directed hydrogen bond placement: Low viscosity amine solvents for CO<sub>2</sub> capture. *ACS Sustainable Chemistry & Engineering*, 7, 7535–7542.  
<https://doi.org/10.1021/acssuschemeng.8b05481>
- Mani, D. & Arunan, E., 2014. The X-C... $\pi$  (X = F, Cl, Br, CN) carbon bond. *The Journal of Physical Chemistry A*, 118, 10081–10089.  
<https://doi.org/10.1021/jp507849g>
- Mazik, M., 2009. Molecular recognition of carbohydrates by acyclic receptors employing noncovalent interactions. *Chemical Society Reviews*, 38, 935–956.  
<https://doi.org/10.1039/B710910P>
- McDowell, S. A. & Joseph, J. A., 2014. The effect of atomic ions on model  $\sigma$ -hole bonded complexes of AH<sub>3</sub>Y (A = C, Si, Ge; Y = F, Cl, Br). *Physical Chemistry Chemical Physics*, 16, 10854–10860.  
<https://doi.org/10.1039/C4CP01074D>
- Munárriz, J., Rabuffetti, F. A. & Contreras-García, J., 2018. Building fluorinated hybrid crystals: Understanding the role of noncovalent interactions. *Crystal Growth & Design*, 18, 6901–6910.  
<https://doi.org/10.1021/acs.cgd.8b01105>
- Murray, J. S., Lane, P., Clark, T. & Politzer, P., 2007.  $\sigma$ -hole bonding: Molecules containing group VI atoms. *Journal of Molecular Modeling*, 13, 1033–1038.  
<https://doi.org/10.1007/s00894-007-0225-4>
- Murray, J. S. & Politzer, P., 2011. The electrostatic potential: An overview. *WIREs Computational Molecular Science*, 1, 153–163.  
<https://doi.org/10.1002/wcms.19>
- Murray, J. S., Lane, P., Clark, T., Riley, K. E. & Politzer, P., 2012.  $\sigma$ -holes,  $\pi$ -holes and electrostatically-driven interactions. *Journal of Molecular Modeling*, 18, 541–548.  
<https://doi.org/10.1007/s00894-011-1089-1>
- Murray, J. S., 2024. The formation of  $\sigma$ -hole bonds: A physical interpretation. *Molecules*, 29, 600.  
<https://doi.org/10.3390/molecules29030600>
- Politzer, P., Lane, P., Concha, M., Ma, Y. & Murray, J., 2007. An overview of halogen bonding. *Journal of Molecular Modeling*, 13, 305–311.  
<https://doi.org/10.1007/s00894-006-0154-7>
- Politzer, P., Murray, J. S. & Concha, M. C., 2008.  $\sigma$ -hole bonding between like atoms; a fallacy of atomic charges. *Journal of Molecular Modeling*, 14, 659–665.  
<https://doi.org/10.1007/s00894-008-0280-5>
- Politzer, P., Murray, J. S. & Clark, T., 2010. Halogen bonding: an electrostatically-driven highly directional noncovalent interaction. *Physical Chemistry Chemical Physics*, 12, 7748–7757.  
<https://doi.org/10.1039/C004189K>
- Politzer, P. & Murray, J. S., 2013. Halogen bonding: An interim discussion. *ChemPhysChem*, 14, 278–294.  
<https://doi.org/10.1002/cphc.201200799>
- Politzer, P. & Murray, J. S., 2017.  $\sigma$ -hole interactions: Perspectives and misconceptions. *Crystals*, 7, 212.  
<https://doi.org/10.3390/cryst7070212>
- Reed, A. E., Curtiss, L. A. & Weinhold, F., 1988. Intermolecular interactions from a natural bond orbital, donor–acceptor viewpoint. *Chemical Reviews*, 88, 899–926.  
<https://doi.org/10.1021/cr00088a005>
- Riel, A. M. S., Rowe, R. K., Ho, E. N., Carlsson, A. C., Rappe, A. K., Berryman, O. B. & Ho, P. S., 2019. Hydrogen bond enhanced halogen bonds: A synergistic interaction in chemistry and biochemistry. *Accounts of Chemical Research*, 52, 2870–2880.  
<https://doi.org/10.1021/acs.accounts.9b00189>
- Riley, K. E., Murray, J. S., Fanfrlík, J., Řezáč, J., Solá, R. J., Concha, M. C., Ramos, F. M. & Politzer, P., 2011. Halogen bond tunability I: The effects of aromatic

- fluorine substitution on the strengths of halogen-bonding interactions involving chlorine, bromine, and iodine. *Journal of Molecular Modeling*, 17, 3309–3318.  
<https://doi.org/10.1007/s00894-011-1015-6>
- Scheiner, S., 2020. The ditetrel bond: Noncovalent bond between neutral tetrel atoms. *Physical Chemistry Chemical Physics*, 22, 16606–16614.  
<https://doi.org/10.1039/D0CP03068F>
- Scheiner, S., 2021. Competition between a tetrel and halogen bond to a common lewis acid. *The Journal of Physical Chemistry A*, 125, 308–316.  
<https://doi.org/10.1021/acs.jpca.0c10060>
- Scheiner, S., 2021. Origins and properties of the tetrel bond. *Physical Chemistry Chemical Physics*, 23, 5702–5717.  
<https://doi.org/10.1039/D1CP00242B>
- Shields, Z. P., Murray, J. S. & Politzer, P., 2010. Directional tendencies of halogen and hydrogen bonds. *International Journal of Quantum Chemistry*, 110, 2823–2832.  
<https://doi.org/10.1002/qua.22787>
- Stasyuk, O. A., Jakubec, D., Vondrášek, J. & Hobza, P., 2017. Noncovalent interactions in specific recognition motifs of protein-DNA complexes. *Journal of Chemical Theory and Computation*, 13, 877–885.  
<https://doi.org/10.1021/acs.jctc.6b00775>
- Wang, W., Ji, B. & Zhang, Y., 2009. Chalcogen bond: A sister noncovalent bond to halogen bond. *The Journal of Physical Chemistry A*, 113, 8132–8135.  
<https://doi.org/10.1021/jp904128b>
- Weiner, P. K., Langridge, R., Blaney, J. M., Schaefer, R. & Kollman, P. A., 1982. Electrostatic potential molecular surfaces. *Proceedings of the National Academy of Sciences USA* 1982, 79, 3754–3758.  
<https://doi.org/10.1073/pnas.79.12.3754>
- Varadwaj, P. R., Varadwaj, A., Marques, H. M. & MacDougall, P. J., 2019. The chalcogen bond: Can it be formed by oxygen? *Physical Chemistry Chemical Physics*, 21, 19969–19986.  
<https://doi.org/10.1039/C9CP03783G>
- Zeng, R., Gong, Z., Chen, L. & Yan, Q., 2020. Solution self-assembly of chalcogen-bonding polymer partners. *ACS Macro Letters*, 9, 1102–1107.  
<https://doi.org/10.1021/acsmacrolett.0c00511>
- Zhuo, H., Li, Q., Li, W. & Cheng, J., 2015. The dual role of pnictogen as Lewis acid and base and the unexpected interplay between the pnictogen bond and coordination interaction in  $H_3N \cdots FH_2X \cdots MCN$  (X = P and As; M = Cu, Ag, and Au). *New Journal of Chemistry*, 39, 2067–2074.  
<https://doi.org/10.1039/C4NJ02051K>